Experimental study of dispersed oil-water flow in a horizontal pipe with enhanced inlet mixing, Part 1: Flow patterns, phase distributions and pressure gradients

Heiner Schümann[1,2]*, Murat Tutkun[3,4], Zhilin Yang[1,5], Ole Jørgen Nydal[1]

[1]Department of Energy and Process Engineering, Technical University of Science and Technology, NTNU, Trondheim, Norway
[2]Multiphase Flow Laboratory, SINTEF Petroleum AS, Trondheim, Norway
[3]Department of Fluid Flow Technology, Institute for Energy Technology, Kjeller, Norway
[4]Department of Mathematics, University of Oslo, Oslo, Norway
[5]Statoil ASA, Research, Development and Innovation, Trondheim, Norway

*Corresponding author, Email: heiner.schumann@ntnu.no

Abstract

The study demonstrates how a disturbance of the flow can affect the pressure gradient and further needs a considerable development length to recover. This is of importance for experimental studies as well as industrial applications. Oil-water experiments were conducted in the Well Flow Loop at the Institute for Energy Technology, Norway. Three different mineral oils (*120 mPa*s*, *60 mPa*s* and *35 mPa*s*) and tap water were used. Input water fractions from *0* to *100%* and mixture velocities up to *1.1 m/s* were tested. A static mixer was installed at the test section inlet to introduce mixing. Comparison with non-premixed data showed that onset of dispersion shifts towards lower mixture velocities when the inlet disturbs the flow. This will also have an impact on the pressure gradient. At low mixture velocities when the flow was semi-dispersed, the influence seems to be most serious. Formation of a dense packed droplet layer is assumed to be a major reason for an increasing pressure gradient. Comparing pressure gradient measurements along the pipe it was found that the development length of the flow was still not reached 200 diameters downstream of the inlet mixer.

1. Introduction

Simultaneous transport of oil and water is common practice in petroleum production systems. Initially stratified flow at sufficiently high flow rate can cause instabilities in the oil-water interface leading to droplet formation and transition to flow dispersion. In a production line, however, an emulsion forms already in the reservoir and disturbances due to processing units such as valves and pumps sustain the dispersion process (Cabellos et al., 2009).

Most experimental work, which can be found in the literature, takes separated flow as a starting point were oil and water are merged using Y- or T-manifolds or something similar (Elseth, 2001; Lovick and Angeli, 2004; Nädler and Mewes, 1997; Plasencia and Nydal, 2010; Trallero et al., 1997). Such inlet devices are expected to not considerably contribute to, or force, the dispersion process. Inlet devices are not standardized.

One might hypothesize that the flow becomes independent of the inlet device sufficiently far downstream of the pipe inlet. Unfortunately the flow development is not documented well in many experimental studies. Nädler and Mewes (1997) and Karabelas (1978) assume developed flow after approximately *600* inner pipe diameter (*D*), based on pressure gradient and droplet size measurements respectively. This is considerably longer than most of the reported data which are taken in shorter test sections. Depending on the situation, the development length might be even longer than *600 D*. Therefore, the history of the flow is crucial and the effect of inlet conditions has to be considered. Inlet history effects were found by for instance Angeli (1996), Ngan (2011), Soleimani (1999) and Mandal et al. (2007). In their studies both flow patterns and pressure gradients were influenced by the inlet.

The main objective of this work is to demonstrate the influence of the inlet device on oil-water flow in multiphase laboratories. This was tested by installing a static mixer at the inlet of the test section. Flow patterns, local phase distributions and pressure gradients were then measured for a range of mixture velocities, U_{mix}, and input water fractions, f_w, and compared with data with comparable experimental conditions but without inlet mixer. Three pressure measurements along the test section help to make a statement on the development of the flow.

Particular focus of this paper should be on a peak in the pressure gradient curve when plotted versus the input water fraction which was observed in several previous studies in the case of semi-dispersed flow (Angeli, 1996; Elseth, 2001; Kumara et al., 2009; Nädler and Mewes, 1997). The authors assumed a partial inversion from oil to water continuous flow in the upper part of the pipe to be the reason for this sudden increase of the pressure gradient, typically occurring for input water fractions $f_w > 0.3$. Such a behavior was also found in our laboratory. We were surprised as a smooth pressure gradient curve was expected for low mixture velocities. The question arose if this jump was caused by flow mixing created in the inlet.

In this study a static mixer was chosen as inlet device as it has a fixed geometry as most manifolds used in experimental studies. The flow disturbance is therewith dependent on the mixture velocity. At the same time the mixer will create a strong inlet mixing effect which is easy to identify.

The study focuses on laboratory conditions and does not try to achieve most realistic field conditions. Therefore a straight horizontal test section and tap water instead of brine were chosen which simplifies the requirements to the infrastructure. This choice also enables to compare the results with previous work by Trallero et al. (1997), Angeli (1996) and Nädler and Mewes (1997) who had similar test conditions.

Trallero et al. (1997) experimentally studied oil-water flow pattern transition, local phase fraction and pressure drop in a *15.54 m* long, *5 cm* inner diameter horizontal pipe. An oil-water system, similar to the one used in this study, with a viscosity ratio of $\mu_o / \mu_w = 29.6$ and density ratio of $\rho_o / \rho_w = 0.85$ was tested. A flow pattern classification with six flow patterns, namely segregated flow (stratified flow without and with mixing at the interface, ST and ST&MI), water dominated dispersed flow (dispersion of oil-in-water and water, Do/w&w, and oil-in-water emulsion, o/w) and oil dominated dispersed flow (dispersion of water-in-oil and oil-in-water, Dw/o, Do/w, and water-in-oil emulsion, w/o), was proposed.

Experiments with and without inlet mixing were documented by Angeli (1996). A low viscosity oil was used in her experiments ($\mu = 1.6$ *mPa*s*), and the pipe inner diameter was rather small ($D = 24$ *mm*). The difference in the pressure gradient between the two cases was significant.

The results by Nädler and Mewes (1997) are of interest for comparison because the entrance nozzle was specially designed to prevent the formation of emulsion and the test section length ($L = 48$ *m*, $D = 59$ *mm*) was long enough to reach fully developed flow.

2. Experimental details

2.1 Well Flow Loop

The experiments were performed in the Well Flow Loop of the Institute for Energy Technology (IFE) in Kjeller, Norway. The closed flow loop has a *25 m* long test section with an inner diameter of $D = 100$ *mm*. The pipe sections are made of transparent PVC. From a gravity oil-water separator in the basement of the building the liquids are pumped separately before mixed at the test section inlet. Centrifugal pumps are used to circulate the liquids. At the end of the test section, the liquids enter a pre-separator before returning to the main oil-water separator. A manual choke valve at the bottom of the pre-separator is used to control the liquid level in the vessel. In this way, backflow of gas in the test section can be prevented. The temperature of the liquids are monitored and regulated by a heat exchanger system. The system can be pressurized up to *10 bar(g)*.

A detailed sketch of the test section is shown by Figure 2. The test section was horizontally aligned at $0 \pm 0.1°$. A simple static mixer was installed at the test section inlet, as seen in Figure 1. Crosswise baffles enhanced mixing and promoted an early transition to dispersed flow. The transparent pipe allowed for visual observation of the flow. Video recordings at approximately *20 m* downstream of the inlet were taken. Differential pressure cells were used to measure the pressure drop over three different sections. A broad beam gamma densitometer, measuring the local phase fractions, was installed *18.88 m* downstream of the inlet. Phase fraction and pressure measurements were averaged over a sampling time of *15 sec*. Further shown in Figure 2 are three traversable FBRM probes (focused beam reflection measurement). These probes were used for in-situ droplet characterization. In order to not disturb the flow, the probes, however, were extracted

when measurements, presented in this paper, were performed. FBRM results are presented by another study (Schümann et al.).

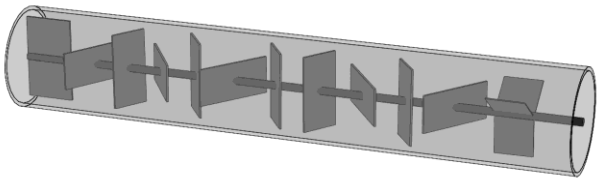

Figure 1: Static mixer at the test section inlet. The flow direction is from left to right.

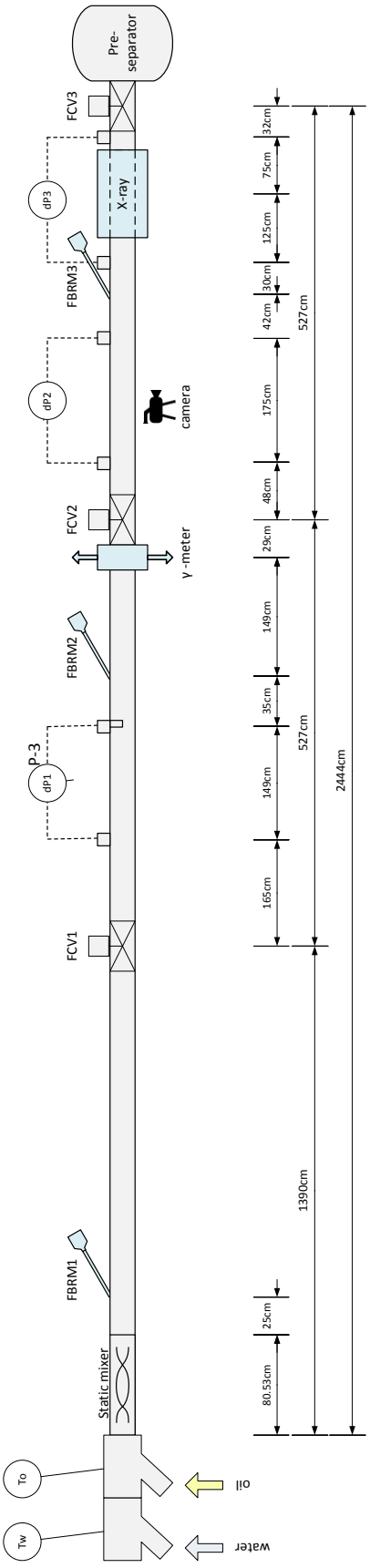

Figure 2: Test section.

2.2 Liquid properties

To investigate the effect of the viscosity on the measured parameters we used three different mineral oil mixtures with different viscosities. All oils were mixtures of Exxsol D80 (μ = *1.7 mPa*s*) and Primol 352 (μ = *165 mPa*s)* and mainly varied in the viscosity. The liquids were mixed by circulating in the flow loop for several hours until property readings were constant as demonstrated in Table 1. Viscosity measurements were completed using an Anton Paar – Physica MCR 301 rheometer. Sample oil was extracted directly from the separator before and after the experiments. The viscosity measurements showed Newtonian behavior. During the experiments the oil density was continuously monitored by Coriolis flow meters. Interfacial tension measurements between water and oil were done with a CAM 200 (KSV Instruments Ltd., Finland) using the pendant drop method.

Table 1: Properties of the tested mineral oil mixtures.

Oil	Composition Primol 352/ Exxsol D80	Density [kg/m^3] (measured at 20°C)	Viscosity [mPa*s] (measured at 20°C)	Interfacial tension with tap water [mN/m] (short/long term)
Oil A	25:1	866 (±0.2%)	120 (±3%)	23/14 (±10%)
Oil B	6:1	859 (±0.2%)	60 (±2%)	23/14 (±10%)
Oil C	4:1	853 (±0.2%)	35 (±2%)	24/15 (±10%)

The temperature of the Well Flow Loop was constantly controlled during the experiments and kept at *20°C* with an accuracy of *±0.5°C*. Arising viscosity changes are considered in the uncertainties given in Table 1.

2.3 Measurement techniques

An electromagnetic flow meter was used to measure the water flow rate. The oil flow rate, however, was measured by Coriolis flow meters. The Coriolis flow meter simultaneously measured the density of the oil as well. When the flow rate is high the retention time of the liquids in the separator could be shorter than the time needed for complete liquid separation. In particular cases we observed that the pumps started to pump an emulsion at high flow rates ($U_{mix} \geq 0.5$ *m/s*). In such cases the permanent monitoring of the density was helpful to identify the water content in the oil. When the water content was distinctively increasing or higher than *2%*, the experiment was stopped. The final input water fraction, f_w, computed from the flow rate measurements, was corrected for the water content in the oil.

Three differential pressure transducers by Fuji Electric (model: FKKW12V1-AKCYY-AE) were positioned along the test section as shown in Figure 2. The *3 mm* diameter pressure tap holes were located at the bottom of the pipe. The impulse pipes from the pressure taps to the DP-cells were filled with water. Before every experiment the impulse pipes and pressure cells were flushed with water to replace possible oil entrainments. The zero point was set at no-flow conditions.

A broad beam gamma densitometer was installed 18.88 m downstream of the test section inlet. It was able to measure 3-phase gas-oil-water flow. In our setup the instrument was used in a 2-phase mode and calibrated once a day. A single value for the overall phase fractions of the scanned cross section was measured.

In addition an X-ray tomography system, that provided more detailed phase fraction data, was installed at the end of the test section, *23 m* from the inlet. With two sources and two detectors in horizontal and vertical alignment respectively, the X-ray tomography system is able to scan the complete cross section of the pipe. The detector-cameras give a resolution better than *1 mm* per pixel. In order to reduce noise groups of neighboring pixels were averaged. The final resolution was *2 mm/pixel*. A sampling frequency of *40 Hz* and sampling times between *10* and *25 sec* were chosen for the experiments. More details on the system can be found in Hu et al. (2014).

Flow patterns were primarily based on visual observations approximately *20 m* (*L/D = 200)* downstream of the mixer. While stratified flow was easy to identify visually the flow became more and more opaque with increasing amount of dispersion. In these cases observations were supplemented by other measurement techniques. Cross sectional reconstructions by the x-ray instrument were useful to investigate the phase distribution inside the pipe. Especially regions free of dispersion could be identified in this way. In fully dispersed flow pressure gradient measurements indicated flow inversion and therewith helped to identify the type of continuity. As described in more detail below, the pressure gradient reaches its maximum at phase inversion which occurs at a specific input water fraction. Water fractions required for phase inversion were found to be in the range between 18% and 30% for the tested oils. Dual continuous flow, where a region of water-in-oil and a region of oil-in-water are present simultaneously could be well identified by a different shading of these regions. The oil-in-water region was typically the darker one.

A major problem was the identification of the type of dispersion in semi dispersed flows for intermediate flow rates. For such flow single droplets were identifiable visually; a distinct interface between an oil and a water continuous region within the dispersion layer, however, as it was the case for dual continuous flow, was only present for the lowest input water fractions and less clear. For higher input water fractions, $f_w > 0.3$, no such a line was observed. We believe that for input water fractions larger than $f_w \approx 0.3$ the dispersion was of type oil-in-water only while for lower input water fractions both types were present. However, in order to not to confuse with speculations we will not further specify the type of dispersion when it was not clear.

2.4 Measurement uncertainties

Uncertainty estimates for pressure gradient and phase fraction measurements following a common root of the sum of the squares method are difficult to perform due to several elemental errors which cannot be tested separately. Uncertainty estimates given here are based on experience and are in good agreement with uncertainties from a simple upper-lower bound method for independent repeatability experiments covering both, single phase and two phase flow. Differences between measurements of equivalent experiments were all within the estimates. All uncertainties are given as absolute uncertainties.

The uncertainty of the pressure measurements is in general much higher than the accuracy of the pressure transducers (*<0.1%*). Typical error sources are drops blocking the impulse

pipes, vibrations of the test rig, flow disturbances or an imperfect pressure tap geometry. An upper limit estimate for the uncertainty of two-phase measurements is given by *max(±7.5%, ±10 Pa/m)*. Also, single phase measurements were compared with theoretical values showing good agreement.

The uncertainty for oil and water phase fraction measurements was *±0.035* using the gamma densitometer.

For X-ray tomography measurements it is more difficult to give an uncertainty estimate. The upper-lower bound method was not applied for this instrument. Comparing the total local phase fractions measured by the gamma densitometer with the x-ray system reveals an agreement more than *93%* between these two instruments. Also, we noticed a difference in the total phase fractions when data from the horizontal and vertical collimators of the x-ray system were compared. Cross sectional information provided by the x-ray system have a high spatial resolution; therefore it gives important qualitative insight into the flow behavior, even though the total phase fraction readings from the broad beam gamma densitometer provide the most accurate data.

3. Test matrix

Mixture velocities up to U_{mix} *= 1.1 m/s* and input water fractions, f_w, varying from *0 – 100 %* (with increments of *10%*) were tested. The mixture velocity was limited by the pumps. Video recordings, pressure drop and local phase fraction measurements were performed for all test cases. We repeated the same test matrix for each oil mixture. A summary is listed in Table 2.

Table 2: Test matrix.

Property	Tested range
Oil viscosity, μ:	35, 60 and 120 mPa*s
U_{mix}:	0.1 – 1.1 m/s
f_w:	0 – 100%

4. Results

4.1 Flow pattern observations

The flow patterns found in this study are in good agreement with flow patterns proposed by Trallero et al. (1997). We chose, however, a further division to better understand the changes in the flow. Figure 3 gives an overview of the observed flow patterns.

Flow pattern maps for oil A, B and C are shown in Figure 4, Figure 5 and Figure 6 respectively. At the lowest mixture velocities the flow was stratified (o&w). Single droplets at the interface could occur. Increasing the mixture velocity resulted in a larger number of droplets. The droplets were still located close to the interface forming a dense packed layer. Turbulence was not strong enough to keep droplets spread over the pipe cross section. A flow pattern sometimes referred to as three-layer pattern, 3L (oil – dispersion – water) occurred (Angeli, 1996; Brauner, 2003; Mandal et al., 2007). The transition criterion from stratified to semi-dispersed flow was a closed droplet layer along the interface. At even higher mixture velocities the droplet layer continued to grow and single droplets were also distributed further away from the interface.

For higher inlet water fractions oil was completely dispersed and the continuous oil phase disappeared. Depending on the mixture velocity, oil droplets were mainly distributed in the upper part (Do/w&w) or spread over the whole pipe cross section for the highest mixture velocities (Do/w). The criterion for the Do/w pattern was based on x-ray measurements showing dispersion present in the whole cross section. In general, as the mixture velocity increases turbulence gains importance compared to the gravitational force. This, in turn, leads to a more uniform distribution of droplets over the cross section. In our case, i.e., premixed flow, this means that turbulence keeps the flow in a dispersed state over a long distance downstream of the mixer. Separation of the phases due to gravitational settling and coalescence is slowed down as the mixture velocity increases.

On the other hand, when the inlet water fraction was low, the free water layer at the bottom of the pipe disappeared. The flow pattern was oil and dispersion (o&D). We observed a stream of fast moving dispersion at the bottom of the pipe and single slower moving droplets in the region above. This could indicate that the dispersion was divided into an oil continuous region and the fast moving water continuous region below. Again, for the highest mixture velocities the phases were not able to separate and the flow was fully dispersed, but this time of the type oil continuous flow (Dw/o).

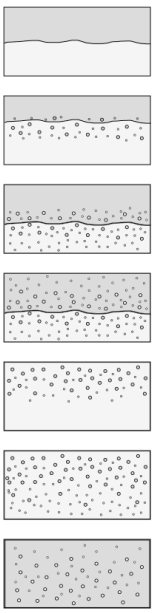

o&w - Stratified flow, single droplets at the interface can occur.

3L (o&D&w) - Three-layer flow: Pure oil and dispersion with a bottom-layer of pure water.

o&D - Oil on top and dispersion in the lower part of the pipe.

Dw/o&Do/w - Dual continuous flow: Water dispersed in oil and oil dispersed in water.

Do/w&w - Dispersed oil in water with a bottom-layer of pure water.

Do/w - Dispersed oil in water.

Dw/o - Dispersed water in oil.

Figure 3: Observed flow patterns.

In fully dispersed state the flow can suddenly transform from oil-in-water to a water-in-oil dispersion and opposite when a certain input water fraction is reached. This is also known as phase inversion and happened for oil A and B when the input water fraction was changed from one to the next measurement point keeping U_{mix} constant. The input water fraction at phase inversion was approximately f_w *= 0.18* for oil A and approximately f_w *= 0.28* for oil B. According to Arirachakaran et al. (1989) the input water fraction at phase inversion decreases with increasing oil viscosity. This is in agreement with our results.

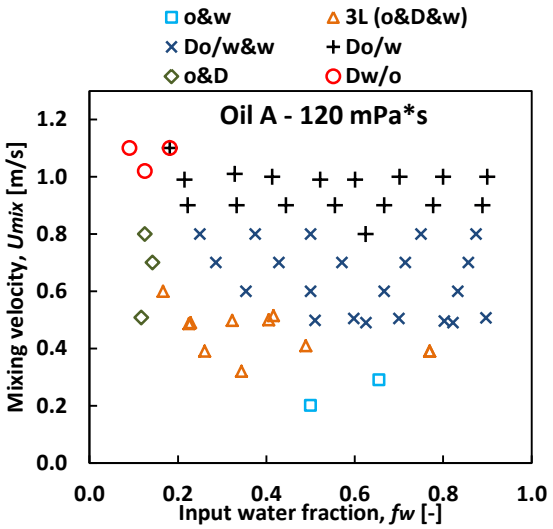

Figure 4: Observed flow pattern map for Oil A - 120 mPa*s.

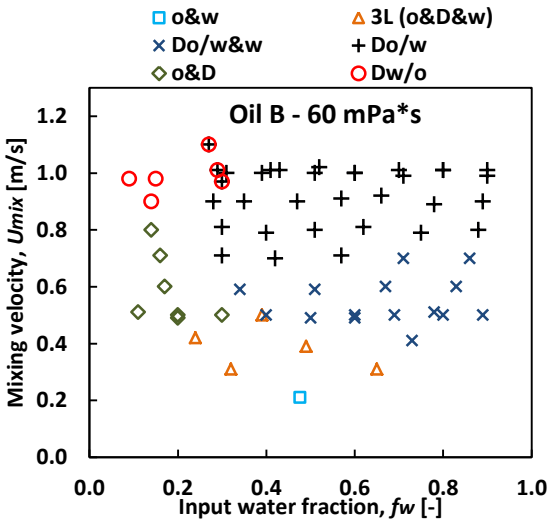

Figure 5: Observed flow pattern map for Oil B - 60 mPa*s.

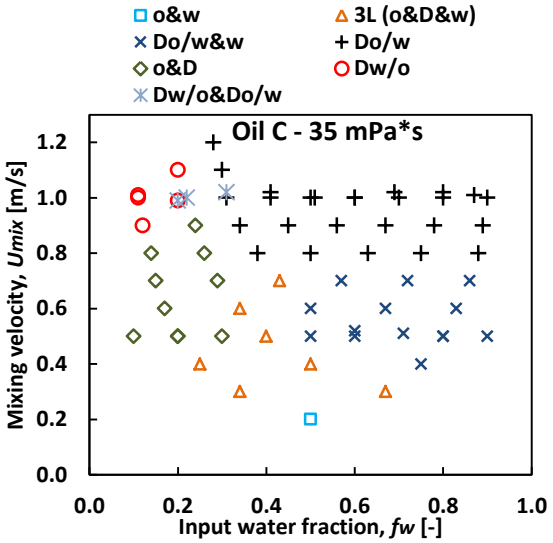

Figure 6: Observed flow pattern map for Oil C - 35 mPa*s.

Phase inversion goes along with a sudden increase of the pressure gradient and was visually observable in the transparent test section. Depending on the initially continuous phase, phase inversion happened in different ways. When the initial flow pattern was Dw/o, we observed a continuous build-up of a Do/w layer (dark shading) from the bottom of the pipe until the complete flow was inverted. The dual-continuous flow pattern was present during the inversion period. On the other side, when the initial flow pattern was Dw/o, the flow seemed to collapse and the phases alternately occupied the pipe (fast alternating dark/bright shading), which was described as intermittent flow by Arirachakaran et al. (1989). After a while the Do/w pattern stabilized. Phase inversion did not occur for oil C. A stable region of dual continuous flow (Dw/o&Do/w) divided the regions of Dw/o and Do/w.

The proposed flow pattern boundaries assembled using the data shown in figures Figure 4, Figure 5 and Figure 6 for oil A, B and C respectively are plotted together in Figure 7. The boundaries move towards higher input water fractions for lower oil viscosities, similar to the input water fractions needed for phase inversion. This can be due to a partly inversion of the dispersed layer also occurring at higher input water fractions. Furthermore, for oil B and C fully dispersed flow of oil-in-water, Do/w, was observed at slightly lower mixture velocities as for oil A. A possible explanation can be found in the work of van der Zande and van den Broek (1998) who measured oil droplets in water in turbulent pipe flow and flow through an orifice. This was attributed to the fact that the viscous oil results in larger energy dissipation during droplet deformation, which leaves less energy for the break-up process, hence the increase of interfacial area. In our experiments, larger droplets produced in the inlet mixer led to a faster separation of the flow.

In general, the minimum mixture velocity needed for the emergence of fully dispersed flow was slightly higher for the oil continuous flow compared to water continuous flow. An even stronger difference was found by Guzhov et al. (1973).

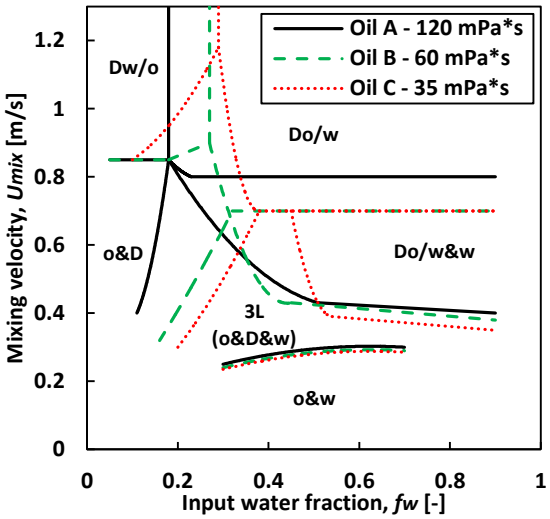

Figure 7: Comparison of observed flow pattern boundaries.

The succession of the observed flow patterns is in good agreement with the flow patterns reported by Trallero et al. (1997) who tested a similar oil-water system. Some discrepancy was found at the boundaries between individual flow patterns. The main difference is the boundary of the stratified region and dispersed flow that appeared at lower

mixture velocities in our study. This can be attributed to two main reasons as we compare the experimental conditions: First, the larger pipe diameter in the presented work will lead to larger Reynolds numbers at equal superficial velocities. Second, the inlet static mixer promotes dispersion even at lower flow rates. As mentioned earlier. The inlet used in the present work differed from the simple Y-junction, which was used by Trallero et al. (1997) to mix the phases. Similar, Angeli (1996) documented that the use of an in-line mixer results in dispersed flow patterns at much lower mixture velocities compared to the same setup without.

Another reason which might be causing the difference between the current work and Trallero et al. (1997) is the interfacial tension. As can be seen in Table 1 the interfacial tension in our work is about *24 mN/m* whereas Trallero et al. reported a value of *36 mN/m*, which is *50%* higher than for our oil.

4.2 Local water fractions

Total local water fractions, measured using the broad beam gamma densitometer, are shown in Figure 8. When U_{mix} *= 1 m/s*, the flow was fully dispersed, and resulting local water fractions are in good agreement with the input water fractions for both oil and water continuous flow. In contrast, at U_{mix} *= 0.5 m/s*, the flow was partly dispersed and local water fractions are below the corresponding input water fractions. Especially for input water fractions larger than *0.4* the oil accumulated distinctively. From f_w *= 0.4* to *0.5* a flow pattern transition was observed. At low input water fraction oil was wetting the upper wall of the pipe. At approximately f_w *= 0.4* a partial inversion (Kumara et al., 2009) of this layer, thus complete dispersion of the oil occurred. At higher input water fractions the flow pattern was a dense packed layer of oil droplets in water on top of a free water layer, Do/w&w. The dispersed oil-in-water layer visually moved considerably slower than the free water, which explains the higher oil accumulation for input water fractions larger than *0.4.*

The measurements were similar for the three tested mineral oils. No significant influence of the viscosity on the total local water fractions was found.

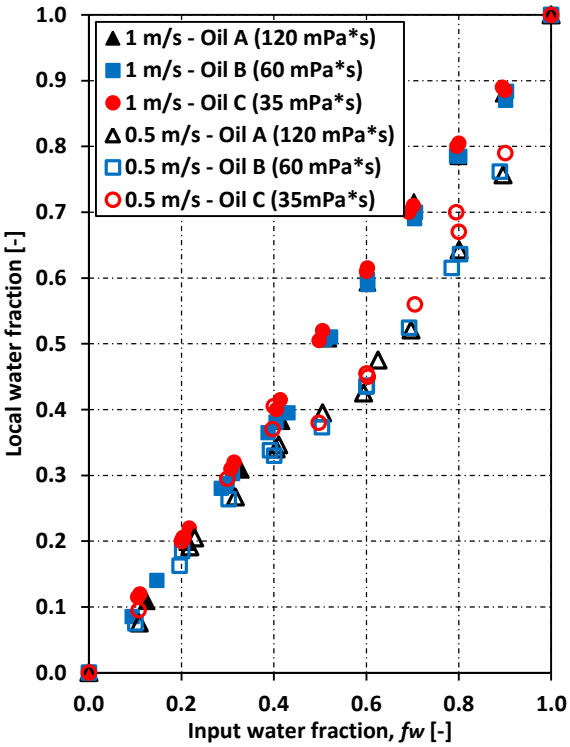

Figure 8: Local water fraction versus input water fraction, f_w, for different mixture velocities.

X-ray data was summarized in line fraction measurements giving the local phase fraction within the pipe (bottom-to-top). Such measurements are shown for oil C (*35 mPa*s*) and the mixture velocities U_{mix} = 1 m/s and U_{mix} = 0.5 m/s in Figure 9 and Figure 10 respectively. Tomographic reconstructions of the total cross sections showing the spatial distribution of the phases are presented in Figure 11 for characteristic cases.

For fully dispersed oil continuous flow (U_{mix} = 1 m/s, f_w *= 0.11* and f_w *= 0.20*) water droplets are rather uniformly distributed over the cross section. In water continuous flow, f_w *> 0.31*, the amount of dispersed oil is continuously increasing towards the top of the pipe. This indicates a faster separation behavior downstream of the inlet mixer when the flow is water continuous. In oil continuous flow the viscosity of the oil will slow down this process. For f_w *= 0.31* the line fraction curve shows a bend in the lower part of the pipe section. This could indicate the interface between the water and oil continuous layer in a dual continuous flow pattern.

For U_{mix} = 0.5 m/s, regions of water, oil and dispersed flow can be clearly distinguished using both the line fraction and cross sectional measurements. In agreement with the visual observations, a pure oil layer was only found for input water fractions of f_w *= 0.4* and below. At f_w *= 0.5*, the line fraction measurements show a dispersed layer of relatively constant water fraction in the upper part of the pipe. This supports the assumption of partial inversion in this region forming a dense packed dispersion layer.

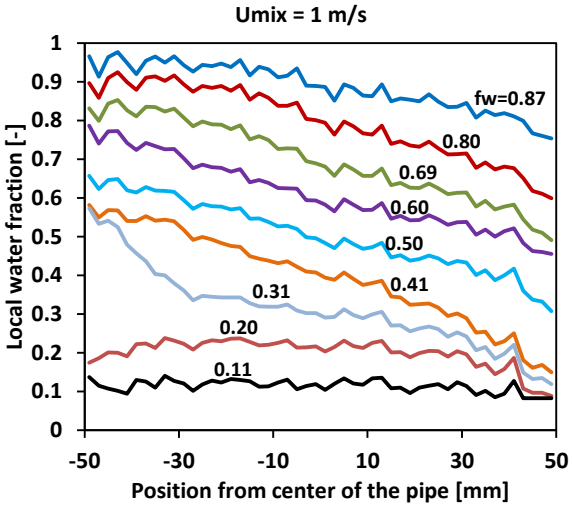

Figure 9: Water line fraction measurements for Oil C (35 mPa*s) at U_{mix} = 1m/s. The input water fractions, f_w, are shown in the figure.

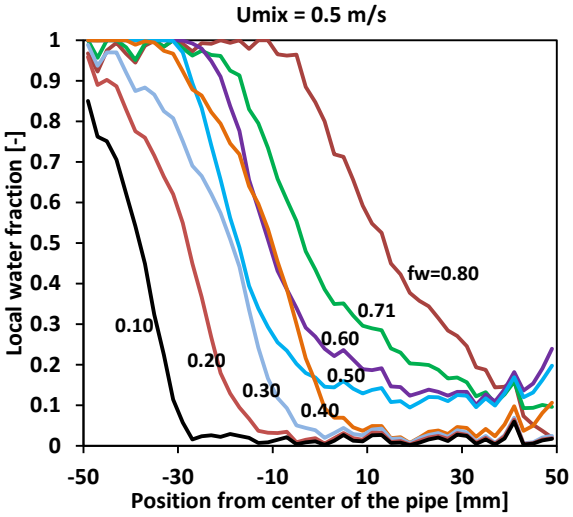

Figure 10: Water line fraction measurements for Oil C (35 mPa*s) at U_{mix} = 0.5m/s. The input water fractions, f_w, are shown in the figure.

.

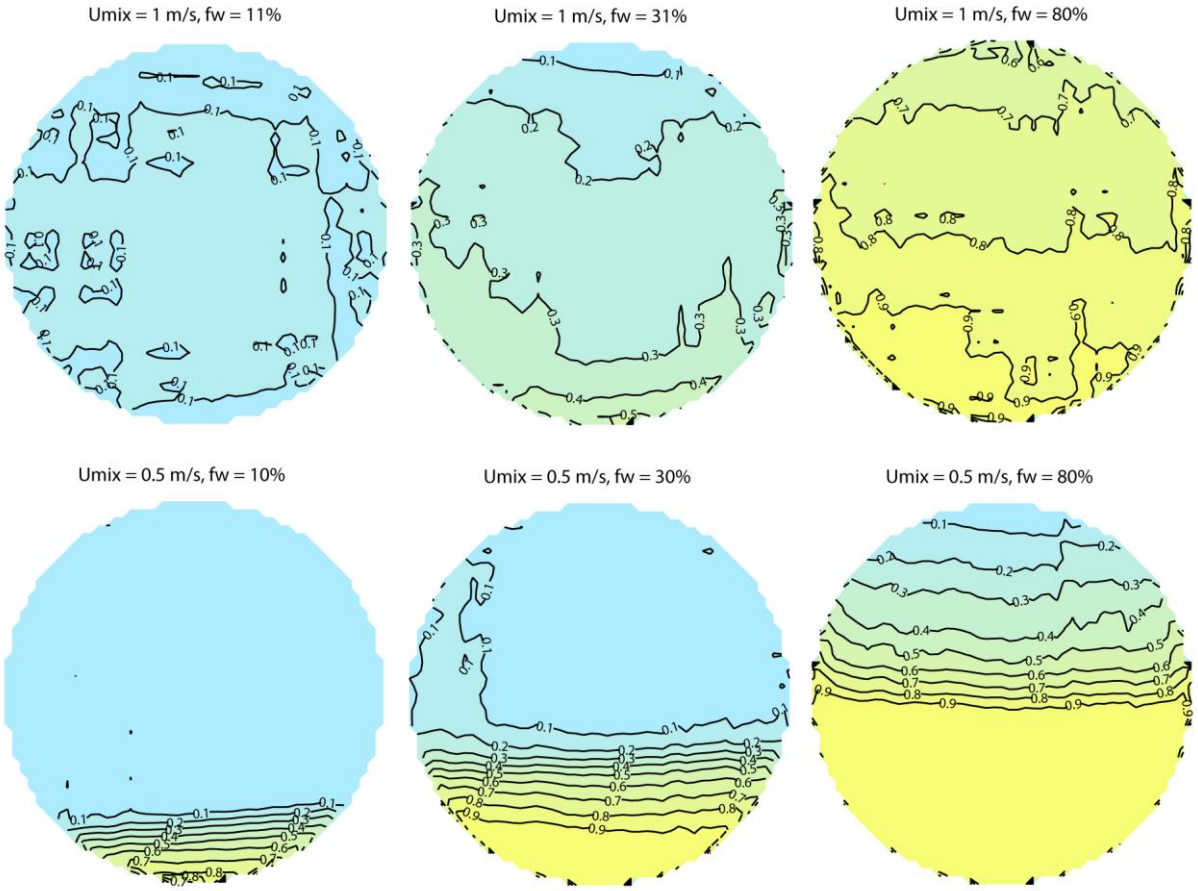

Figure 11: Tomographic reconstruction of the cross sectional water distribution for oil C (35 mPa*s). Contour lines show the local water fraction in steps of 0.1.

From the cross sectional plot, Figure 11 (U_{mix} = *0.5 m/s*, f_w = *80%*), we find a region in the upper part of the dense packed droplet layer where the local water fraction falls below that at phase inversion. We tried to better identify the type of dispersion by suddenly stopping the flow, using fast closing valves, and observing the stagnant separation behavior. Droplets started to arrange by size developing a gradient in droplet size with the largest droplets on top. From visual observations of the flow and the separation behavior we got

the impression of the dispersion being of type oil droplets in water.

Also droplet deformation was observed in this dense packed layer which would allow for closer packing. The pipe wall blocks further upward movement. As explained in Merchuk et al. (1998) droplets in this situation queue up and wait for coalescence to take place

4.3 Oil-water pressure drop

Figure 12 shows pressure gradients for U_{mix} = *1 m/s* and U_{mix} = *0.5 m/s* measured using the second pressure transducer at *200 D* downstream of the inlet.

At U_{mix} = *1 m/s* the pressure gradient increases toward a peak in the phase inversion region, which is well documented in the literature (Angeli and Hewitt, 1999; Arirachakaran et al., 1989; Nädler and Mewes, 1997; Pal, 1993). As mentioned earlier, oil C does not show a direct phase inversion. Instead, the flow crosses a dual-continuous flow region, Dw/o&Do/w. Also in this case a peak is shown.

Comparing the different oils, we found that the pressure gradient for oil-continuous flow increases with increasing oil viscosity. In contrast, the water-continuous flow does not show a dependency on the oil viscosity. This is in agreement with measurements by Arirachakaran et al. (1989).

Lovick and Angeli (2004) reported a drag reduction effect for both oil and water continuous flow. This was attributed to dynamic coalescence and breakup processes reducing turbulence in unstable dispersions as explained by Pal (1993). According to our results it, however, is clear that a higher dispersed phase concentration increased the pressure drop. Only for oil C, the lowest viscosity case, a drag reduction effect was found when the flow is oil continuous. Single phase flow of oil C at Umix = 1m/s provides a Reynolds number of Re= 2429. This indicates that the flow is in a transitional regime which can be sensitive to drag reduction effects.

The viscosity dependency of the pressure gradient shows a similar behavior for U_{mix} = *0.5 m/s*. For input water fractions less than *0.4* when an oil continuous layer was present, the flow was sensitive to the oil viscosity. Here a drag reduction was found when a higher water fraction increased the water wetted perimeter. This effect was stronger for higher oil viscosities.

The flow pattern transition to Do/w&w between f_w = *0.4* and f_w = *0.5* goes along with a sudden increase in the pressure gradient as the oil continuous layer disappears. With a further increase in f_w the observed dense packed droplet layer becomes thinner and, in turn, the pressure gradient decreases. Again, no significant influence of the oil viscosity was found, which would be expected assuming that oil was completely dispersed. A peak at partial inversion was documented in the literature for both non-premixed flow (Angeli, 1996; Elseth, 2001; Kumara et al., 2009; Nädler and Mewes, 1997), and premixed flow (Angeli, 1996). This indicates that the effective viscosity in the dense packed layer, now wetting the upper part of the pipe, exceeds that of pure oil. The increase in pressure is in accordance with the oil accumulation found in section 4.3.

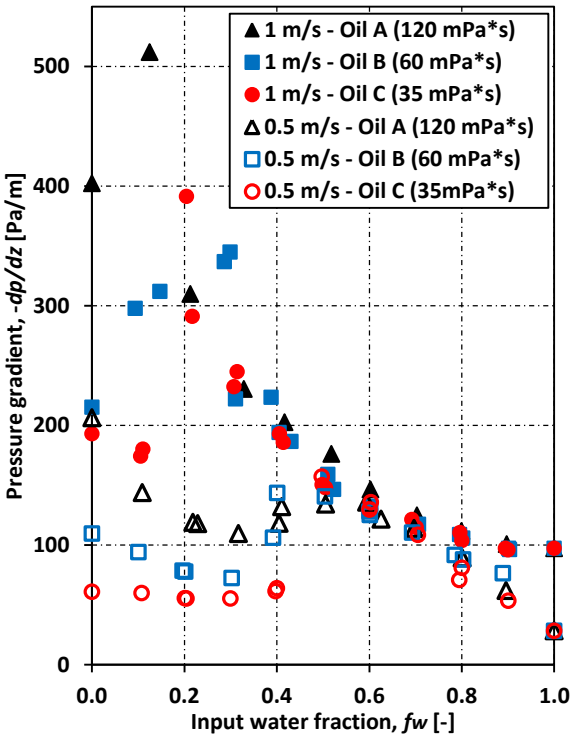

Figure 12: Pressure gradient versus input water fraction, f_w.

Interestingly, for *0.5* < f_w < *0.8* the pressure gradient reached similar values for U_{mix} = *0.5 m/s* as for U_{mix} = *1 m/s*. At U_{mix} = *1 m/s*, inlet mixing creates a relatively homogeneous droplet distribution over the cross section which prevails downstream the pipe. At U_{mix} = *0.5 m/s*, the weak dynamics of the flow allow fast droplet settling and form the dense packed droplet layer with a very high effective viscosity, probably exceeding this of homogenous flow strongly. This is an interesting result as the practical meaning would be a larger amount of transported liquid without increasing the pumping power in this case. The same result was found when further mixture velocities were considered (Figure 13). The reason behind this observation is not entirely clear. Further experiments with different inlet mixing rates would be necessary to understand if the coinciding lines are characteristic for inlet mixing or just coincidence. However, from Figure 13 we can further investigate that the partial inversion and thus the peak in the pressure gradient moves towards lower input water fractions for higher U_{mix}.

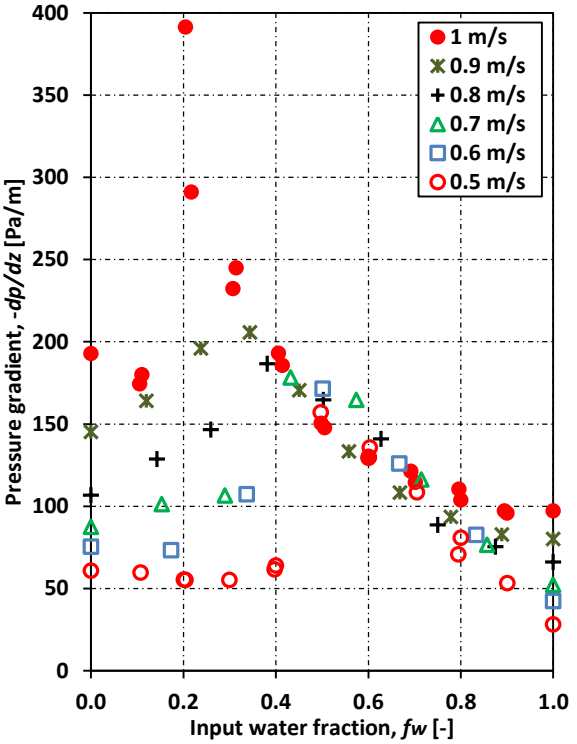

Figure 13: Pressure gradient versus input water fraction, f_w, for oil C and different U_{mix}.

5. Comparison with non-premixed data

Results for oil B (*60 mPa*s*) were compared with experimental data (*69 mPa*s*) from a previous measurement campaign conducted at the same facility, but without the static mixer installed at the inlet. Both oils are mixtures of the same base oils. The viscosities differ to some degree which introduces an uncertainty in the comparison. However, we will allow for a qualitative comparison of the data, as we have shown before that the influence of the viscosity is limited and the relative viscosity difference is small. Similar to the presented experiments, also in the previous measurement campaign different oil viscosities, covering a range from *69* to *153 mPa*s* were tested. Again, measurements repeated for different oil viscosities were collapsing when oil was dispersed (e.g. Do/w and Do/w&w). Differences due to viscosity were only observed when oil formed a continuous layer, but were small compared to differences when the flow pattern was changed as a result of inlet mixing, which will be shown below.

Line fraction measurements for the non-premixed experiments at U_{mix} = *1 m/s* and *0.5 m/s* are shown in Figure 14 and Figure 16. Pressure gradient measurements for both cases are compared in Figure 15 and Figure 17.

From Figure 14 we observe that for measurements of f_w > *0.3* the local water fraction shows a steep gradient from pure water at the bottom of the pipe to an approximately constant low value in the upper part of the pipe, which is significant for a dense packed dispersion. The flow pattern is Do/w&w. Premixed flow at U_{mix} = *1m/s* was more homogeneous with a weak gradient in the water line fraction. Comparing the pressure gradient measurements (Figure 15), with inlet mixer the more homogeneous dispersion resulted in lower pressure gradients when the flow was water continuous. It was further found that phase inversion, identified by a peak in the pressure gradient, takes place at slightly higher input water fractions when a mixer was installed. Alteration of the phase inversion point as result of inlet mixing was also found by Soleimani (1999).

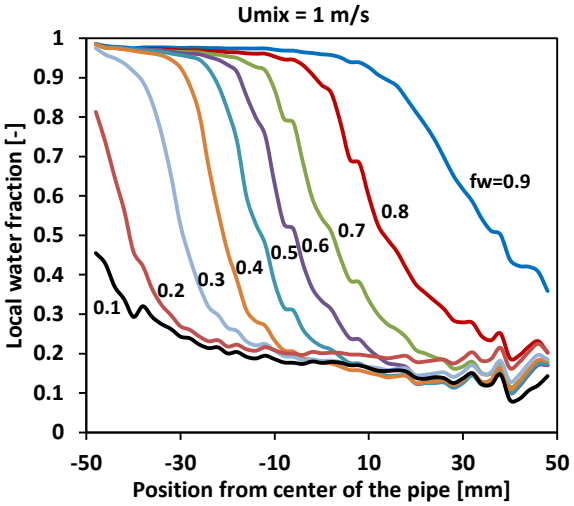

Figure 14: Water line fraction measurements at U_{mix} = *1m/s* without inlet mixing (69 mPa*s). The input water fractions, f_w, are shown in the figure.

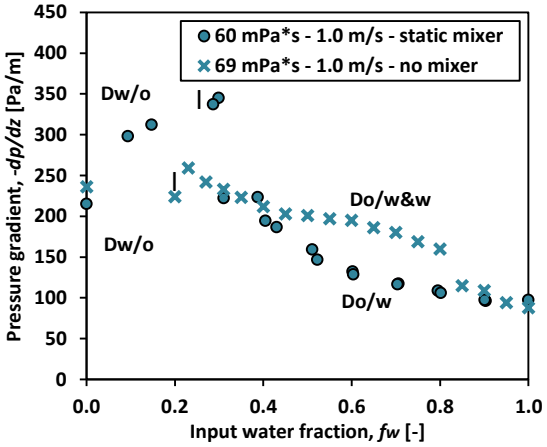

Figure 15: Comparison of pressure gradient measurements with and without inlet mixing at U_{mix} = *1 m/s*. The X-axis shows the input water fraction, f_w.

At U_{mix} = *0.5 m/s* the same flow patterns were found with and without mixer. As before, the line fraction gradient is steeper for the non-premixed case. This indicates a thin dispersion layer in the 3L flow pattern. Also the input water fraction required for flow pattern transition (partial phase inversion) was different. For input water fractions smaller than *0.4* the pressure gradient is almost identical. At f_w = *0.4* the 3L flow pattern (oil-dispersion-water) changes to Do/w&w in the premixed case and the pressure gradient rises dramatically. This transition happens at much higher input water fraction, f_w = *0.8* without the inlet mixer. Also in this case, the partial inversion goes along with a jump in the pressure gradient, but less dramatic as with the mixer.

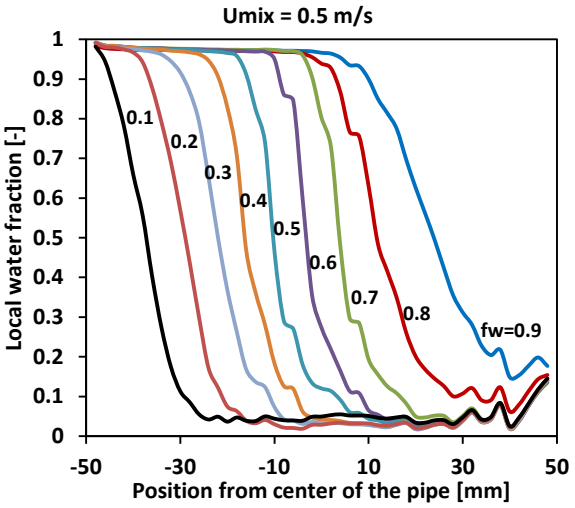

Figure 16: Water line fraction measurements at U_{mix} = 0.5m/s without inlet mixing (69 mPa*s). The input water fractions, f_w, are shown in the figure.

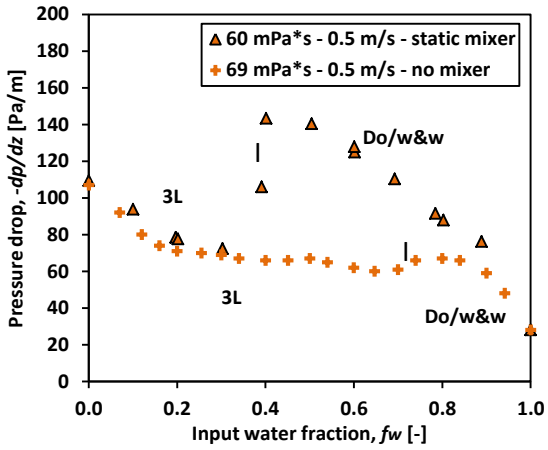

Figure 17: Comparison of pressure gradient measurements with and without inlet mixing at U_{mix} = 0.5 m/s. The X-axis shows the input water fraction, f_w.

Our measurements agree with findings of Soleimani (1999), who measured a substantial pressure increase for water dominated flow, while the measurements for oil dominated flow stayed constant when a mixer was used.

Similar results were found when pressure gradient data with and without inlet mixing of Angeli (1996) were plotted together in Figure 18. The mixer used was a STATIFLOW in-line static mixer. The data shows that the effect of inlet mixing also applies when low viscosity oil is used.

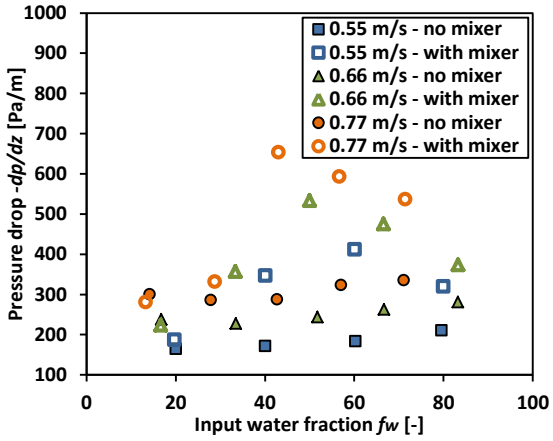

Figure 18: Comparison of pressure gradient measurements with and without inlet mixing. The X-axis shows the input water fraction, f_w. Data extracted from (Angeli, 1996). μ = 1.6 mPa*s, ID = 24 mm.

6. Flow development

Flow development along the pipe was found by comparing pressure gradient measurements at three different positions. Figure 19 displays these measurements for oil B (*60 mPa*s*) at U_{mix} = *1 m/s*. The trend is not clear in the case of oil continuous flow (f_w < *0.29*.) The local pressure gradient increases from the first to the second pressure transducer and decreases from the second to the third pressure transducer. For water continuous flow the pressure gradient was gradually decreasing further downstream the pipe. This trend is clear, even considering the measurement uncertainty mentioned before. Trends were similar for oil A and C (not shown). Also for U_{mix} = *0.5 m/s* the trend was decreasing for the major part of the cases.

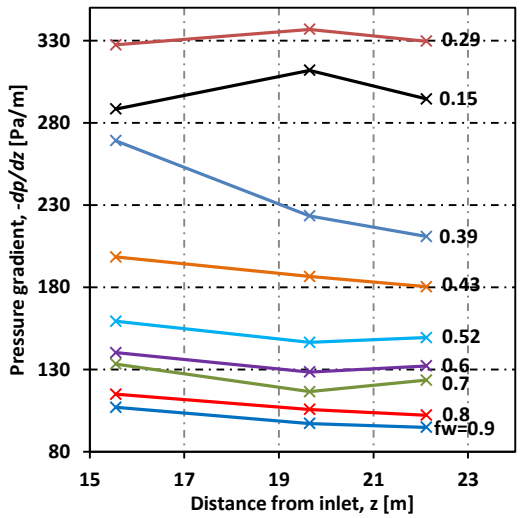

Figure 19: Pressure gradient along the pipe for oil B (60 mPa*s) at U_{mix} = 1 m/s. Different lines represent different input water fractions, f_w.

The development length of the flow will depend on the velocity and initial mixing. In premixed flow three main mechanisms, namely turbulence decay, droplet settling and droplet coalescence will be important where coalescence most likely has the longest time scale. Especially in water continuous flow the low viscosity of the water is not expected to restrict droplet settling considerably when droplets

overcome turbulent diffusion or the flow is laminar. As mentioned before several experiments were abruptly stopped in order to investigate the stagnant separation behavior. The stagnant separation behavior cannot be adopted to flow development not considering the dynamics of the flow. However, here we can consider it for the simplest estimate. As an example the separation time for the flow pattern Do/w&w at U_{mix} = *0.5 m/s* and f_w = *0.7* after stopping was over four minutes. Considering U_{mix} = *0.5 m/s* this would correspond to a developing length of over *120 m* or *L/D = 1200* which is considerably longer than the test section. Separation experiments in separate beaker-mixer tests showed that the total separation time is one order of magnitude higher than the settling time. This would explain the formation of a thick dense packed layer in premixed flow as it was observed for semi dispersed flow in this study. Pal (1996) found that droplet growth reduces the emulsion viscosity which is in agreement with the decreasing pressure gradient measurements.

7. Conclusion

Horizontal oil-water pipe flow experiments using different oil viscosities (*120 mPa*s*, *60 mPa*s* and *35 mPa*s*) were presented. With help of a static inlet mixer the phases were premixed and developed further downstream toward a less mixed or separated flow pattern. Comparison with experimental studies using a simple Y- or T-junction as inlet manifold showed that the flow is sensitive to the inlet. If the inlet device promotes mixing of the flow, transition to dispersed flow was observed at lower mixture velocities. This has an impact on the frictional pressure gradient. In the case of low mixture velocities, when the flow was semi dispersed, higher pressure gradients were measured with inlet mixing. Especially a pressure gradient peak appearing at the transition from 3L-flow to Do/w&w when the inlet water fraction was increased was amplified. Furthermore, this transition shifted towards lower input water fractions. At higher mixture velocities when the flow is fully dispersed mixing provides more homogenous flow. Higher pressure gradients were measured at low input water fractions and lower pressure gradients at higher input water fractions compared to non-premixed flow.

Changing pressure gradient measurements along the pipe showed that fully developed flow was not yet reached after L/D = 200. Also for non-premixed experiments the literature reports considerable developing lengths (L/D = 600) (Nädler and Mewes, 1997).

As consequence of limited test section lengths in experimental studies the inlet section should be chosen carefully. Possible influence on the flow has to be considered. Also the state of flow development should be investigated and reported. This has further impact on model development and comparison. Data from several studies is probably not suitable for evaluating point models predicting developed steady state flow.

Even if the presented experiments have been conducted under simplified laboratory conditions some conclusions can be drawn regarding practical problems of oil production. In real crude oils natural or added emulsifiers can be present (Kokal, 2005). Enhanced mixing of the flow caused by for instance pumps and valves can be expected to persist considerably longer than for mineral oils without surface active agents. Depending on the infrastructure the impact of a resulting higher pressure gradient over the development length of the flow for example would be limited if the total transport length is long (many kilometers). However, additional mixing of the flow can be problematic at the end of a production line. When a choke valve is installed shortly before the flow enters a separator more dispersion or a finer droplet size could influence the subsequent separation of the fluids. A larger required volume or even different type of the separator can be consequences (Lim et al., 2015; van der Zande and van den Broek, 1998).

8. Acknowledgements

The authors acknowledge the financial support from The Multiphase Flow Assurance Innovation Centre (FACE). FACE is a research cooperation between IFE, NTNU and SINTEF. The center is funded by The Research Council of Norway and by the following industrial partners: Statoil ASA, GE Oil & Gas, SPT Group - A Schlumberger Company, FMC Technologies, CD-adapco, Shell Technology Norway.

9. References

Angeli, P., 1996. Liquid-liquid dispersed flows in horizontal pipes. Ph.D. Thesis. Imperial College of Science, Technology and Medicine, London

Angeli, P., Hewitt, G.F., 1999. Pressure gradient in horizontal liquid-liquid flows. Int J Multiphas Flow 24, 1183-1203. http://dx.doi.org/10.1016/S0301-9322(98)00006-8

Arirachakaran, S., Oglesby, K.D., Malinowsky, M.S., Shoham, O., Brill, J.P., 1989. An Analysis of Oil/Water Flow Phenomena in Horizontal Pipes. SPE Production Operations Symposium, Oklahoma City. Society of Petroleum Engineers. http://dx.doi.org/10.2118/18836-MS

Brauner, N., 2003. Liquid-Liquid Two-Phase Flow Systems, Modelling and Experimentation in Two-Phase Flow. Springer Vienna, pp. 221-279.

Cabellos, E.M., Carvalho, M.S., Ponce, R.V., 2009. Oil-in-water emulsion formation in laminar flow through capillaries. 20th International Congress of Mechanical Engineering, Gramado.

Elseth, G., 2001. An Experimental Study of Oil / Water Flow in Horizontal Pipes. Ph.D. Thesis. Telemark University College, Porsgrunn

Guzhov, A.I., Grishin, A.D., Medvedev, V.F., Meved-eva, O.P., 1973. Emulsion Formation During the Flow of Two Liquids in a Pipe. Neftianoe Khoziastvo Oil Industry 8, 58-61.

Hu, B., Langsholt, M., Liu, L., Andersson, P., Lawrence, C., 2014. Flow structure and phase distribution in stratified and slug flows measured by X-ray tomography. Int J Multiphas Flow 67, 162-179. http://dx.doi.org/10.1016/j.ijmultiphaseflow.2014.06.011

Karabelas, A.J., 1978. Droplet size spectra generated in turbulent pipe flow of dilute liquid/liquid dispersions. AIChE Journal 24, 170-180. DOI: 10.1002/aic.690240203

Kokal, S., 2005. Crude-Oil Emulsions: A State-Of-The-Art Review. SPE Production & Facilities 20, 5-13.

Kumara, W.A.S., Halvorsen, B.M., Melaaen, M.C., 2009. Pressure drop, flow pattern and local water volume fraction measurements of oil-water flow in pipes. Measurement Science and Technology 20, 1-18. http://dx.doi.org/10.1088/0957-0233/20/11/114004

Lim, J.S., Wong, S.F., Law, M.C., Samyudia, Y., Dol, S.S., 2015. A review on the effects of emulsions on flow behaviours and common factors affecting the stability of emulsions. Journal of Applied Sciences 15, 167-172. 10.3923/jas.2015.167.172

Lovick, J., Angeli, P., 2004. Experimental studies on the dual continuous flow pattern in oil-water flows. Int J Multiphas Flow 30, 139-157. http://dx.doi.org/10.1016/j.ijmultiphaseflow.2003.11.011

Mandal, T.K., Chakrabarti, D.P., Das, G., 2007. Oil Water Flow Through Different Diameter Pipes: Similarities and Differences. Chemical Engineering Research and Design 85, 1123-1128. http://dx.doi.org/10.1205/cherd06036

Merchuk, J.C., Andrews, B.A., Asenjo, J.A., 1998. Aqueous two-phase systems for protein separation, Studies on phase inversion. Journal of Chromatopraphy B: Biomedical Sciences and Applications 711, 285-293. http://dx.doi.org/10.1016/S0378-4347(97)00594-X

Ngan, K.H., 2011. Phase inversion in dispersed liquid-liquid pipe flow. Ph.D. Thesis. Unviversity College London, London

Nädler, M., Mewes, D., 1997. Flow induced emulsification in the flow of two immiscible liquids in horizontal pipes. Int J Multiphas Flow 23, 55-68. http://dx.doi.org/10.1016/S0301-9322(96)00055-9

Pal, R., 1993. Pipeline Flow of Unstable and Surfactant-Stabilized Emulsions. AIChE Journal 39, 1754-1764. DOI: 10.1002/aic.690391103

Pal, R., 1996. Effect of Droplet Size on Rheology of Emulsions. AIChE Journal 42, 3181-3190. DOI: 10.1002/aic.690421119

Plasencia, J., Nydal, O.J., 2010. Influence of the pipe diameter in dispersed oil-water flows. 7th International Conference on Multiphase Flow, Tampa.

Schümann, H., Tutkun, M., Nydal, O.J., Experimental study of dispersed oil-water flow in a horizontal pipe with enhanced inlet mixing, Part 2: In-situ droplet measurements. submitted to the Journal of Petroleum Science and Engineering.

Soleimani, A., 1999. Phase distribution and associated phenomena in oil-water flows in horizontal tubes. Ph.D. Thesis. Imperical College Lodon, London

Trallero, J.L., Sarica, C., Brill, J.P., 1997. A Study of Oil/Water Flow Patterns in Horizontal Pipes. SPE Production & Facilities 12, 165-172. http://dx.doi.org/10.2118/36609-PA

van der Zande, M.J., van den Broek, W.M.G.T., 1998. Break-up of oil droplets in the production system. Proceedings of ASME Energy Sources Technology Conference and Exhibition, Housten.